Published in final edited form as:
Sens Actuators B Chem. 2010 June 3; 147(2): 714–722. doi:10.1016/j.snb.2010.03.029.

Dually Fluorescent Sensing of pH and Dissolved Oxygen Using a Membrane Made from Polymerizable Sensing Monomers

Yanqing Tian[1,*], **Bradley R. Shumway**[1], **A. Cody Youngbull**[1], **Yongzhong Li**[1], **Alex K.-Y. Jen**[2], **Roger H. Johnson**[1], and **Deirdre R. Meldrum**[1]

[1] Center for Ecogenomics, Biodesign Institute, Arizona State University, Tempe, AZ 85287

[2] Materials Science & Engineering, University of Washington, Seattle, WA 98195

Abstract

Using a thermal polymerization approach and polymerizable pH and oxygen sensing monomers with green and red emission spectra, respectively, new pH, oxygen, and their dual sensing membranes were prepared using poly(2-hydroxyethyl methacrylate)-co-poly(acrylamide) as a matrix. The sensors were grafted on acrylate-modified quartz glass and characterized under different pH values, oxygen concentrations, ion strengths, temperatures and cell culture media. The pH and oxygen sensors were excited using the same excitation wavelength and exhibited well-separated emission spectra. The pH-sensing films showed good response over the pH range 5.5 to 8.5, corresponding to pK_a values in the biologically-relevant range between 6.9 and 7.1. The oxygen-sensing films exhibited linear Stern-Volmer quenching responses to dissolved oxygen. As the sensing membranes were prepared using thermally initiated polymerization of sensing moiety-containing monomers, no leaching of the sensors from the membranes to buffers or medium was observed. This advantageous characteristic accounts in part for the sensors' biocompatibility without apparent toxicity to HeLa cells after 40 hours incubation. The dual-sensing membrane was used to measure pH and dissolved oxygen simultaneously. The measured results correlated with the set-point values.

Keywords

optical sensors; dual sensors; pH sensor; oxygen sensor; membranes; polymerizable sensing monomers

1. Introduction

Simultaneous detection of pH and dissolved oxygen concentrations is important for monitoring drinking water qualities, determining freshness of food, and understanding cell metabolism, cell respiration rate, cell health and diseases including cancer. Many pH and oxygen sensors have been developed based on monitoring electro-chemical or optical (color, emission

[*] To Whom all correspondence should be addressed: yanqing.tian@asu.edu; Phone: 1-480-965-9601; Fax : 1-480-727-6588.

Supplementary data: Reversibility of the pH sensor film at pH 3 and 9, temperature effect on pH sensing film, oxygen response of the oxygen sensing membrane in DMEM medium, cytotoxicity, and short term photostability of the pH and oxygen sensing films were given as supplementary materials.

intensity, or lifetime) response [1-3]. In general, two separate sensors have to be applied in parallel to simultaneously measure pH and oxygen concentration.

Optical sensors are minimally or non-invasive, disposable, can be fabricated at microscale dimensions and combined with optical fiber for remote measurement of (bio)chemical parameters, and allow for imaging of oxygen tension over a surface or in volume [4]. To date, several fluorescence-based smart optical dual pH and oxygen sensors have been developed [4-8]. These dual sensors are usually based on fluorescein-derivatives as pH sensors and platinum porphyrins as oxygen sensors physically dispersed in suitable polymer matrices. Klimant and Wolfbeis groups studied a few excellent dual sensors and applied their sensors for real samples measurements, including in natural marine sediments [7] and bacterial growth in 24 well microplates [8]. Using their dual optical sensor systems, Klimant group obtained highly reliable results when used in the marine samples, which are quite close to the results measured using pH and dissolved oxygen electrodes [7]. Wolfbeis group demonstrated that the dual pH and dissolved oxygen optical sensors are suitable for parallelized, miniaturized bioprocessing, and cell-based high-throughput screening applications with multianalyte detection versatility [8].

Platinum (II) and palladium (II) porphyrins [9-12], are typical fluorescence-based oxygen sensors. Advantages of these materials include their long triplet-state lifetimes (in a range of 20 to 70 microsecond) and sufficient triplet-triplet energy transfer from these compounds to oxygen molecules, resulting in a decrease of the oxygen sensors' emission intensities, a shortening of their lifetimes by oxygen, and generation of singlet oxygen. These porphyrin derivatives are usually physically trapped in various polymer matrices including silicon rubbers or gels, polystyrene, cellulose derivatives, and polyurethane-type hydrogels [4-12]. A potential drawback associated with physical trapping is leaching of probes from the matrix when submersed in aqueous solutions [5,13] This is especially problematic with protracted soaking in cell culture medium at 37°C, since leaching may cause inaccurate measurements and cytotoxicity. In order to alleviate this problem, it is necessary to chemically link the oxygen probes to the polymer matrix.

Recently, Payne et al. developed a new oxygen sensor based on Ruthenium(II) star polymer with the sensing probe chemically conjugated with polystyrene. Using this approach, the leaching of sensor was avoided [14]. The oxygen probes used in this work is a monomer with a platinum porphyrin unit (**M1**,Figure 1), which emits in the red spectral window, can be polymerized with other monomers, and can be grafted onto glass substrates with suitable glass surface modifications. In order to prepare dual sensing membranes with integrated pH sensing ability (requiring high ion permeability), poly(2-hydroxyethyl methacrylate) (PHEMA)-containing hydrogel was chosen as the matrix (e.g. the membrane). The PHEMA-containing hydrogel possesses excellent mechanical, chemical and thermal stability; exhibits good oxygen and proton permeability; and is transparent and biocompatible, being widely used for contact lenses [15,16].

Various materials are suitable as fluorescence-based optical pH sensors based on different sensing mechanisms, including intramolecular charge transfer, photo-induced electron transfer (PET), and excited state intramolecular proton transfer [17,18]. Among the many optical pH sensors, 4-amino-1,8-naphthalimide fluorophore-based pH sensors are known to have high quantum yields, satisfactory selectivity and reproducibility, sufficient stability and short response time [19,20]. For this study, a 4-amino-1,8-naphthalimide-containing chromophore (**M2**), a green emitter, was chosen as the pH sensor. This sensor is also a monomer, enabling its grafting onto glass substrates by polymerization to form stable membranes. As the lifetime of the naphthalimide type pH sensor is shorter than 10 nanoseconds and its emission is mainly from the singlet excited state [21,22], quenching by oxygen is negligible. Therefore, in the dual

sensing system, the pH sensor can serve as an internal reference for the oxygen sensor. The oxygen sensor is a neutral platinum porphyrin without pH response group, and serves as an intra-reference for the pH sensor. The two monomers, **M1** and **M2**, were reported previously [23–25], however, herein they were first time studied in the PHEMA hydrogel thin films and integrated together as dual pH and oxygen sensors. These two sensors can be excited at the same wavelength, but emit their luminescence at different wavelengths. By taking advantage of the characteristics of the two chosen sensors, a ratiometric method [26–30] is applicable for the determination of pH and oxygen concentration in a dual-sensing system, and is expected to be a more practical approach for biological applications. Although pH values and oxygen concentrations can be determined using the intensity change of an individual pH or oxygen sensor, in practical applications intensity measurements based on a single sensor are often adversely affected by instrumental conditions and external interferences including fluctuations in source intensity, dye concentration and background fluorescence. In order to alleviate these problems a ratiometric measurement method was developed based on the intensity ratios or lifetimes of two different fluorescent dyes in the sensor layer, one sensitive to the analyte and the other used as a reference. The ratiometric approach lends itself to easy operation and/or provides enhanced signal stability and accuracy [26–30].

We are aiming to integrate the optical sensors with lab-on-a-chip devices for single cell metabolism studies [31,32]. Herein, we report the performance of individual pH-, oxygen- and dual-sensing membranes in pH buffers and medium under a variety of experimental conditions, including dissolved oxygen concentration, pH, ion strength and temperature. We also evaluated the toxicity of the sensing films to HeLa cancer cells.

2. Experimental section

2.1 Materials and reagents

All chemicals and solvents were of analytical grade and were used without further purification. The oxygen (**M1**) and pH (**M2**)-sensing monomers were prepared according to known procedures [23–25]. 3-(4,5-Dimethylthiazol-2-yl)-2,5-diphenyltetrazolium bromide (MTT), *N*,*N*′-dimethylformamide (DMF), trimethylsilylpropyl acrylate (TMSPA), 2-hydroxyethyl methacrylate (HEMA), azobisisobutyronitrile (AIBN), and acrylamide were obtained from Aldrich (St. Louis, MO). Ethyloxylate trimethylolpropane triacrylate (SR454®) was purchased from Sartomer (Exton, PA). Double-distilled water was used to prepare the buffer solutions. The pH values were determined with a digital pH meter (Thermo Electron, Beverly, MA) calibrated at room temperature (23 ± 2 °C) with standard buffers of pH 10.01, 7.00 and 4.01. Britton-Robinson (B-R) buffers composed of acetic acid, boric acid, phosphoric acid and sodium hydroxide were used to tune the pH values. Calibration gases (nitrogen and oxygen, each of 99.999% purity) were purchased from AIR Liquide America, LP (Houston, TX). Gas mixtures were precisely controlled with a custom-built, in-line, digital gas flow controller. All sensing measurements were carried out at atmospheric pressure, 760 mmHg or 101.3 kPa. A temperature controller was used to adjust the temperature from 23 to 37 °C using a Fisher Scientific Isotemp 202S water bath with ± 0.5 °C precision. Dulbecco's Modified Eagle's Medium (DMEM, Invitrogen, Carlsbad, CA) was tuned to pH values in the range of 3.5 to 10.0 by the addition of HCl or NaOH aqueous solution. Quartz glass from University Wafer (South Boston, MA) was cut into squares of 13.1 × 13.1 mm and 3.6 × 3.6 mm using a dicer (Microautomation, Billerica, MA).

2.2 Instruments

An oxygen plasma cleaner (Harrick Plasma, Ithaca, NY) was used for quartz substrate surface activation. A Shimadzu RF-5301 spectrofluorophotometer (Shimadzu Scientific Instruments, Columbia, MD) was used for fluorescence measurements. To facilitate measurements of the

films in liquid solutions, quartz substrates (13.1 × 13.1 mm) coated with sensor layers were inserted across the diagonal into 1-cm optical path quartz fluorescence cuvettes with 3 mL of pH- and temperature-controlled buffer solutions to enable the sensing membrane to be positioned at an angle of 45° to the excitation light. A micro DO electrode (Model DO-166FT, Lazar Research Laboratories, inc. Los Angeles, CA) was used to measure the dissolved oxygen concentration in B-R buffers.

2.3 Glass surface modification

In order to achieve stable polymer-membrane coating, the quartz surface was modified with the acrylate-containing silane, TMSPA. The quartz glass was detergent cleaned and sonicated in isopropanol, then treated with oxygen plasma for approximately 30 minutes to generate active hydroxyl groups. The quartz glass was immediately placed in a vacuum chamber for 20 hours to graft a thin layer of TMSPA to its surface using a known vapor deposition method [33].

2.4 Preparation of polymer membrane stock solutions

The sensor monomer (**M1**, or **M2** or both **M1** and **M2**) (1 mg for **M2**, and/or 5 mg for **M1**), HEMA (800 mg), acrylamide (200 mg), SR454 (50 mg), and AIBN (10 mg) were dissolved in 1 mL DMF (for the oxygen sensor, 10% $CHCl_3$ was used as a co-solvent with DMF to increase **M1**'s solubility).

2.5 Polymer membrane preparation

10 μL of the stock solution was pipetted onto the surface of the TMSPA-modified quartz substrate and covered with a clean cover slip (untreated) to form a sandwich structure. The thickness was controlled using a *25*-μm Kapton tape shim (DuPont, Wilmington, DE). The substrate-sensor-cover slip sandwich was placed in a vacuum oven, which was then evacuated and flushed three times with dry nitrogen gas. Polymerization was carried out under nitrogen at 80 °C for 1.5 hours. More detailed polymerization was described in the results section. The substrates with polymerized membranes were taken out of the oven, and the tape and cover slip removed. The membranes were washed three times in methanol and three times in double distilled water to remove any residual monomer and DMF. The films were dried and stored in the dark at room temperature.

3. Results and discussion

3.1 Polymer membrane preparation

To produce polymer membranes with good mechanical stability and oxygen permeability, hydrophobic SR454 was chosen as a crosslinker. An increase in hydrophobic segments in PHMEA increases oxygen permeability [15,16]. To further increase the water and ion permeability, acrylamide was added as a second monomer for the membrane formation [19, 20]. Thermal polymerization of the monomers (sensors, HEMA, acrylamide and SR454) in DMF under nitrogen using AIBN as an initiator was used to form hydrogels on the quartz surface, in order to avoid photo-bleaching of the sensors [34] that may occur when short wavelength (365- or 254-nm) is used for photopolymerization. The reaction was performed at 80°C under nitrogen to decrease the polymerization time. Under these conditions, uniform and stable polymer membranes on quartz surfaces were obtained after 1.5 hr.

3.2 pH sensor study

3.2.1 Properties of pH sensing membranes in B-R buffers at room temperature

—Figures 2A and 2B show the absorbance and emission spectra of a pH sensing membrane. Bathochromic shifted absorbance spectra were observed from acidic to basic condition. Similar

results were observed in other 4-amino-1,8-naphthalimide-containing pH sensing films [19, 20, 23, 24]. Fluorescence intensity increased with a decrease in pH value. This result is ascribed to photo-induced electron transfer (PET) in the pH sensors being suppressed by the protonation of the amino group. When a fluorophore is attached to an electron quencher (usually one or more nitrogen-containing functional groups which are non-conjugated to the fluorophore), PET occurs between them [17, 19, 20, 35]. In the piperazinyl group of **M2**, the nitrogen atom (NCH_3) is not directly connected to the 4-amino-1,8-naphthalimide fluorophore, of which the NCH_3 moiety is a strong electron donor. PET occurs from the lone electron pair of the NCH_3 group to the acceptor naphthalimide fluorophore, making the sensor weakly fluorescent. At lower pH, however, the protonation of the amino group diminishes the PET effect and, in turn, leads to restoration of the fluorescence originating from the fluorophore, 4-amino-1,8-naphthalimide. Hence, a remarked increase in emission intensity was observed at low pH. The typical dynamic range of pH response was from 8.5 to 5.5. The fluorescence intensity changes are described well by a sigmoidal function (Boltzmann fitting) as shown in equation 1.

$$\frac{I}{I_0}=\frac{m1-m2}{1+\exp(\frac{pH-pK_a'}{p})}+m2 \quad (1)$$

where, I and I_0 are the fluorescence intensities measured at varying pH values and at the highest pH value (pH 10) used during the calibration, respectively. $m1$, $m2$, pK_a', and p are empirical parameters describing the initial value ($m1$), the final value ($m2$), the point of inflection (pK_a'), and the width (p) of the sigmoidal curve. The fluorescence intensity changes and their curve fittings are shown in Figure 2C. The apparent pK_a value (pK_a') was 7.04 for the pH sensing film in B-R buffers without any addition of sodium chloride. The fitting was highly reliable with a correlation coefficient (R^2) of 0.999. Thus, the pH sensing membrane, having a pK_a close to 7, is expected to be suitable for applications in medicine and biotechnology.

3.2.2 Salt influence on pH sensing—For the pH sensing, one important factor is the influence of ion strength on the dissociation constant, and consequently the pK_a of the sensor. Figure 2C shows intensity ratio changes of the same pH sensing membrane in buffers of different ionic strengths with various sodium chloride concentrations. The pK_as were 7.04, 7.00, 7.03 and 7.09 for 0 mM, 1 mM, 10 mM and 100 mM NaCl in the B-R buffers respectively. The influence of ionic strength on sensing performance and cross-sensitivity of the pH sensing membrane to ionic strength were both negligible.

3.2.3 Response time and leaching—Response time of the sensing membrane, t_{95} (i.e. the time for 95% of the total change in fluorescence intensity to occur), to a change in pH was less than 1 minute in the transition from pH 8.5 to pH 3.5, and less than 2 minutes in the reverse direction. This response time is similar to optical pH sensors based on sol-gel silica and polymer gel matrices [1,5,19,20,36]. Since the probes were polymerized with other monomers in the membranes and the membranes were chemically grafted on the quartz surfaces, leaching of the probes from the membranes was not observed when soaking in PBS buffer at room temperature for 24 hr. The sensor film also had a good reversibility, which was tested for 6 cycles between pH 9 and pH 3 (see S-Figure 1 of supplementary data).

3.2.4 pH response in DMEM—Because cellular and biological analyses often take place in cell culture medium, the performance of the sensor was tested in DMEM. A typical titration of the sensing film in DMEM with various pH values at room temperature is shown in Figures 2D and 2E. Because the medium contains many additives, including amino acids, sugars, phenol red and serum, which may quench the pH sensors, the fluorescence intensity at a given

pH in DMEM is approximately 25% weaker than that in B-R buffer of the same pH. Because of the influence of the additives in DMEM as well as autofluorescence, the emission peak of the pH sensor shifted approximately 10 nm at high relative to low pH. An additional peak from 550 – 625 nm, which belongs to the autofluorescence of the medium, was also observed. The intensity ratio of low pH (3.5) to high pH (10) was 21, greater than the ratio in B-R buffer (~14), indicating higher sensitivity in the medium than in B-R buffer. The pK_a value (6.82) in medium remained close to 7, although lower than those in B-R buffers. Therefore, the sensing membrane is expected to be suitable for pH determination in cell culture medium.

For pH study, the matrix must be ion permeable. Therefore, the sensors easily interact with the solutes in aqueous media, which may affect the probe's behaviors. The interferences often occur in the liquid systems. In order to alleviate this problem, there are two possible methods. (1) Sensors may be designed to be slightly hydrophobic in order to reduce the interactions of the sensing moieties with the additives in the media. However, the design needs a rationization in order to not alter the sensors responses, pK_a values, and application ranges significantly. (2) Matrices can also be tuned. Still, the influence of the matrices on the sensing performance needs to be evaluated. Electrodes do not suffer the interference problems. However, the electrode can not be used for noninvasive study in biological samples nor are they suitable for small volumes (a few tens pL) for single cell study.

3.2.5 Temperature effect on pH sensing membrane—Temperature is an important factor affecting emission intensities. To quantify this effect, fluorescence intensities at pH 5.5 and 7.5 were measured under varying dissolved oxygen concentrations at 25, 28, 31, 34, and 37 °C (see S-Figure 2 in supporting information). The intensity of the sensing membranes decreased with increasing temperature. Oxygen concentration had no effect on the fluorescence intensity of the pH sensor. The fluorescence quenching by increased temperature is more significant at low pH than at high pH. Thus, temperature should be controlled in order to obtain accurate pH measurements.

3.2.6 Photostability and lifetime of pH sensing membrane—To investigate the photostability of the sensor, the sensing membrane in pH 7.50 B-R buffer was continuously exposed to 405-nm excitation light (0.2 mW/cm^2) for a period of 5 h. The membrane fluorescence intensity was recorded at 2-min intervals. A 2.9% intensity decrease was observed consequent to the integrated expose, which corresponded to a variation of 0.02% per measurement. It is important to consider photobleaching in organic chromophores. 4-amino-1,8-naphthalimide-containing pH sensors are more stable than fluorescein-containing pH sensors [19]. The sensing membrane was found to have a lifetime of at least four months when stored in water at room temperature in the dark. Covalent immobilization of the active component in the copolymer significantly reduces the leaching effect, improving sensors' lifetime.

3.3 Oxygen sensor study

3.3.1 Response of oxygen sensing membrane—Figure 3 shows the response of an oxygen sensing film measured in B-R buffer (pH 7.5) at room temperature. Typical platinum porphyrin Soret and Q-bands were observed at 403, 510 and 591 nm (Figure 3A). The absorbance spectra were unaffected by dissolved oxygen, indicating there was no chemical reaction between the dissolved oxygen molecules and the platinum porphyrin fluorophores. A marked dependence of fluorescence intensity on dissolved oxygen concentrations was observed (Figure 3B), showing that the emission of the probes was physically quenched by oxygen, and that the sensor membrane exhibited high oxygen permeability in aqueous solution.

The intensity ratios (I_0/I) curve (Figure 3D) follows the Stern-Volmer equation:

$$\frac{I_0}{I} = 1 + K_{SV}[O_2] \quad (2)$$

where K_{SV} is the Stern-Volmer quenching constant and $[O_2]$ is the dissolved oxygen concentration [37,38]. I_0 and I are the steady-state fluorescence signals measured in the presence of nitrogen and various oxygen concentrations generated by controlled gas bubbling, respectively. The dissolved oxygen concentration $[O_2]$ is proportional to the partial pressure of oxygen, pO_2, in the gas used to saturate the liquid. At 23 °C under air condition with the oxygen partial pressure of 21.3 kPa, the $[O_2]$ in the B-R buffer is 8.6 mg L^{-1}.

The fluorescence intensity ratio in the absence and presence of air, $I_0/I_{8.6}$, was approximately 2.6 at room temperature. This ratio is comparable to those reported for oxygen sensing films with pltatinum porphyrins physically trapped in polymer matrices of polystyrene and poly (styrene-*block*-vinylpyrrolidine) nanobeads [5,9,34]. Equation 2 fits the experimental data with correlation coefficients exceeding 0.996. Many realized oxygen sensing films, hydrogels, and silica particles consisting of the oxygen sensors physically trapped in the matrix do not have linear Stern-Volmer constants. This nonlinearity may be due to non-uniform distribution or aggregation of sensor materials within the matrix [4–7,34]. The linear response of the oxygen sensing membrane in aqueous solution indicates a uniform distribution of the sensing moiety in the thin films achieved by a solution polymerization preparation method. Obata et al. [25] reported a non-linear Stern-Volmer response to oxygen when the sensing monomer **M1** was physically trapped in poly(isobutyl-co-2,2,2-trifluoroethyl methacrylate) matrix. Linear response was observed when films were prepared from a copolymer containing the sensing moiety **M1**.

3.3.2 Temperature effect on oxygen sensing—In contrast to pH, which had negligible influence on the sensitivity of the membranes to oxygen, temperature was observed to significantly affect the oxygen response of the membrane. Figures 3C and 3D show the temperature dependence of the oxygen sensing membrane in B-R buffers at 23, 27, 32, and 37°C. As with the pH sensing membranes, emission intensities were decreased slightly at higher temperatures under a given oxygen partial pressure (Figure 3C). The oxygen quenching effect is more pronounced at higher temperature (Figure 3D). The increase in sensitivity of the oxygen sensor at high temperatures has been reported previously [1, 5, 7, 39, 40], and is likely due to enhanced interaction of oxygen molecules with sensing moieties.

3.3.3 Oxygen sensing in DMEM—To monitor biological processes, the sensing membranes must also be functional in cell culture medium at 37°C. The oxygen quenching effect in DMEM medium equilibrated with oxygen/nitrogen mixed gas in a range of oxygen partial pressure of 0 – 30 kPa at 37°C was studied (see S-Figure 3 in supporting information). Because of the many additives in the medium the fluorescence intensity of the membrane in DMEM was approximately 50% lower than in B-R buffer. The response of the membrane to oxygen still followed the first-order linear Stern-Volmer equation. At 37°C, the Stern-Volmer quenching constant in DMEM (0.067 kPa^{-1}) is much less than in B-R buffer (0.106 kPa^{-1}). An additional weak peak from DMEM autofluorescence was observed at 550-620 nm.

3.3.4 Temporal response of oxygen sensing membrane—The response time of the membrane in buffer (pH 7.5 was chosen as a biologically-relevant case) to oxygen was short. The response time (t_{95}) to change from air-saturated buffer to deoxygenated B-R buffer and back was less than 10 seconds in both cases. Although faster-responding sensors have been reported [41,42], this sensor's response time was faster than some other sol-gel materials [43, 44], making it a viable option for monitoring oxygen response in biological applications. The

sensor film also had a good reversibility, which was tested for 6 cycles between deoxygenated solutions and oxygenated solutions.

3.3.5 Photostability of oxygen sensing membrane—The sensing membrane in buffer solution at pH 7.50 was continuously exposed to excitation light at 405 nm over a period of five hours, while fluorescence intensity was recorded at two-minute intervals. A total intensity fall-off of 4.6% was observed with a decrease of 0.03% per measurement. Under the same excitation conditions, the oxygen sensor was observed to have less stability than pH sensor reported here. Photostability enhancements are now in progress.

3.4 Dual sensor films study

Similar to the preparation of single sensor-containing membranes, the dual sensors were prepared by polymerization of the HEMA/acrylamide/SR454/DMF solution with both monomers, **M1** and **M2**. Because the pH sensor had no response to dissolved oxygen concentration, and the oxygen sensor was not influenced by pH, each can be used as a reference for the other. Using the same excitation wavelength (e.g. 405 nm), their emissions had no significant overlap. The response can be calculated from their individual emission changes or by the ratiometric approach. Figures 4A and 4B show the effect of changes in dissolved oxygen concentration and pH on the fluorescence intensities of the dual sensors. Fluorescence intensity changes and their ratios for the dual sensor film are shown in Figures 4C and 4D. Two approaches were used for the pK_a and K_{SV} determinations. One approach utilized the emission intensity changes of the individual sensors in Equations 1 and 2 to determine pK_a and K_{SV}. pK_a determination using the emission intensity at 515 nm of the pH sensor in Equation 1 will be called method A, and K_{SV} determination using the oxygen sensor emission intensity change at 660 nm in Equation 2 will be called method B. Another approach is to use intensity ratios of the two sensors using Equation 1 (called method C) for pK_a determination and Equation 2 (called method D) for K_{SV} determination. In method C, I_0 is the emission intensity peak at 660 nm (due to the oxygen sensor), which is an intra-reference for the emission intensity, I, at 515 nm (due to the pH sensor). In method D, I_0 is the emission intensity at 515 nm, which is an intra-reference for the emission intensity, I, at 660 nm.

Whether method A or method C was used, the pH sensing intensity followed a sigmoidal Boltzmann relationship. The calculated pK_as using the two different methods are nearly identical (Table 1), proving the robustness of the ratiometric approach. The high reliability is attributable to the immunity of the pH sensor to oxygen concentration changes, and of the oxygen sensor to pH change, the lack of overlap between the two sensors' emission spectra, and the need for only one excitation wavelength equalizing the exciting energy.

Whether method B or method D was used, simple Stern-Volmer response of the oxygen sensing moiety to oxygen molecules was observed. Because of the different definition of I_0 in methods B and D, the K_{SV}s from the two approaches are not comparable.

The construction of the dual sensor films may have influenced the pK_a and K_{SV} values. The dual sensor film showed a slightly lower pK_a than that of the pH sensor alone and higher K_{SV} than that of the oxygen sensor alone. This may be due to fluorescence resonance energy transfer (FRET) [45,46] from the pH to the oxygen sensor, as the emission of the pH sensor has an overlap with the absorbance of the oxygen sensor.

3.5 Validation

The response functions of the pH sensor were validated with test solutions of pH 5.53, 7.16, and 7.60 at pO_2 of 21 kPa. The oxygen response functions were tested in pH 7.5 buffers equilibrated with oxygen and nitrogen gas mixtures with 5, 8, 10, 12, 15, and 20% of oxygen

corresponding to pO_2 of 5.1, 8.1, 10.1, 12.2, 15.2 and 20.2 kPa. Experiments were performed at room temperature using the dual sensing membrane. The results are given in Table 2. The numbers in parentheses are deviations of the measurements from the set-point values of the test solutions. Both pH measurement methods gave satisfactory results with experimental pH value errors less than ±0.16. Both oxygen measurement methods yielded results within ±10% of the set-points. This dual-sensing membrane appears to be reproducible and suitable for practical application.

3.6 Cytotoxicity study

Cytotoxicity to HeLa cancer cells was investigated using MTT-based toxicology assay kit. Detailed experiment was given in supporting information. No significant inhibition of cell proliferation or cytotoxicity was observed after 40 hours incubation in the presence of the sensing membranes, demonstrating excellent biocompatibility of the new sensing membranes.

3.7 Discussion of advantages and disadvantages of the sensor systems reported herein

Using chemical immobilization of the sensing moieties in the hydrophilic PHEMA matrix, no leaching of the sensing moieties was observed. With this chemical polymerization approach using multi-monomers with different sensing capacities, devices for multi-parameters measurements can be successfully fabricated. This approach enhances the application of the sensing films for monitoring multiple biological parameters in an environment. Disadvantages were also observed as: (1) there were significant decreases in intensity of the pH sensors and oxygen sensors on going from standard B-R buffers to cell culture mediums, (2) pK_a and K_{SV} changes were also observed from the B-R buffers to cell culture mediums, and (3) FRET was observed in dual sensor films, which shifted the pK_a of the pH sensor and of K_{SV} oxygen sensor in going from the single sensor to dual sensors. These shortcomings may results in experimental errors when applied in unknown sample matrices. Further endeavors are necessary to alleviate these problems. Suitable matrices, which can minimize interactions of the probes with media, need to be explored. Interference by media is a problem as it often occurs but is not always completely removed. Using the lifetime measurement approach rather than intensity method will also be studied as it is believed that lifetime is less affected by experimental conditions, which will reduce experimental errors. Individual sensor chemically immobilized in nanoparticles with these particles chemically immobilized in a certain matrix to keep the probes apart may reduce or eliminate the FRET, as it is known that efficient FRET occurs within 10 nm between the donor and acceptor pair.

4. Conclusion

New pH, oxygen and dual-sensing membranes were prepared and tested over biologically-relevant pH, temperature, ion strength, and oxygen concentration ranges in B-R buffers and cell culture medium. The typical dynamic pH response was observed between pH 5.5 and 8.5. pK_as of the sensing films were around 7, and only slightly affected by the cell culture medium and buffers. Oxygen response in the hydrogels followed the linear Stern-Volmer equation. The pH sensor was unaffected by oxygen concentration, and the oxygen sensor did not respond to pH changes. Thus, each may provide an intra-reference for the other in dual-sensing membranes. Sensor films were made from polymerizable monomers and probes did not leak from the membrane matrix into buffers or cell culture medium. No cytotoxicity was observed using the MTT assay, indicating excellent biocompatibility of the films. These sensing membranes are being applied to single-cell metabolism studies.

Supplementary Material

Refer to Web version on PubMed Central for supplementary material.

Acknowledgments

Financial support was provided by the Microscale Life Sciences Center, an NIH Center of Excellence in Genomic Sciences at Arizona State University: Grant 5P50 HG002360. We also thank Dr. Nam Seob Baek for the platinum porphyrin precursor synthesis.

References

1. Borisov SM, Nuss G, Klimant I. Anal Chem 2008;80:9435–9442. [PubMed: 19006407]
2. Yotter RA, Lee LA, Wilson DM. IEEE Sensors J 2004;4:395–411.
3. Yotter RA, Lee LA, Wilson DM. IEEE Sensors J 2004;4:412–429.
4. Wolfbeis OS. J Mater Chem 2005;15:2657–2669.
5. Vasylevska GS, Borisov SM, Krause C, Wolfbeis OS. Chem Mater 2006;18:4609–4616.
6. Nagl S, Wolfbeis OS. Analyst 2007;132:507–511. [PubMed: 17525805]
7. Schröder CR, Polerecky L, Klimant I. Anal Chem 2007;79:60–70. [PubMed: 17194122]
8. Kocincova AS, Arain SN, Krause C, Borisov SM, Arnold M, Wolfbeis OS. Biotechnol Bioeng 2008;100:430–438. [PubMed: 18383124]
9. Lee SK, Okura I. Anal Commun 1997;34:185–188.
10. Köse ME, Carrol BF, Schanze KS. Langmuir 2005;21:9121–9129. [PubMed: 16171341]
11. Borisov SM, Vasylevska AS, Krause C, Wolfbeis OS. Adv Funct Mater 2006;16:1536–1542.
12. Kimura F, Khalil G, Zettsu N, Xia Y, Callis J, Gouterman M, Dalton L, Dabiri D, Rodriguez M. Meas Sci Technol 2006;17:1254–1260.
13. Butler TM, MacCraith BD, McDonagh C. J Non-Cryst Solids 1998;224:249–258.
14. Payne SJ, Fiore GL, Fraser CL, Demas JN. Anal Chem 2010;82:917–921. [PubMed: 20050641]
15. Fornasiero F, Krull F, Prausnitz JM, Radke CJ. Biomaterials 2005;26:5704–5716. [PubMed: 15878376]
16. Wang Y, Tan G, Zhang S, Guang Y. Applied Surface Science 2008;255:604–606.
17. Valeur, B. Molecular Fluorescence: Principles and Applications. New York: Wiley; 2002.
18. Tian YQ, Chen CY, Yang CC, Young AC, Jang SH, Chen WC, Jen AKY. Chem Mater 2008;20:1977–1987.
19. Niu CG, Zeng GM, Chen LX, Shen GL, Yu RQ. Analyst 2004;129:20–24. [PubMed: 14737578]
20. Niu CG, Gui XQ, Zeng GM, Yuan XZ. Analyst 2005;130:1551–1556. [PubMed: 16222379]
21. Gan J, Chen K, Chang CP, Tian H. Dyes and Pigments 2003;57:21–28.
22. Chen G, Wang L, Zhang J, Chen F, Anpo M. Dyes and Pigments 2009;81:119–123.
23. Shen L, Zhu W, Meng X, Guo Z, Tian H. Sci China Ser B-Chem 2009;52:821–826.
24. Tian H, Gan J, Chen K, He J, Song QL, Hou XY. J Mater Chem 2002;12:1262–1267.
25. Obata M, Tanaka Y, Araki N, Hirohara S, Yano S, Mitsuo K, Asai K, Harada M, Kakuchi T, Ohtsuki C. J Polym Sci Part A: Polym Chem 2005;43:2997–3006.
26. Song A, Parus S, Kopelman R. Anal Chem 1997;69:863–867. [PubMed: 9068274]
27. Xu H, Aylott JW, Kopelman R, Miller TJ, Philbert MA. Anal Chem 2001;73:4124–4133. [PubMed: 11569801]
28. Kermis HR, Kostov Y, Harms P, Rao G. Biotechnol Prog 2002;18:1047–1053. [PubMed: 12363356]
29. Schaeferling, M.; Duerkop, A. Springer Series on Fluorescence Vol 5, Standardization and Quality Assurance in Fluorescence Measurements I. Springer; 2008. p. 373-414.and references therein
30. Lee S, Ibey BL, Cote GL, Pishko MV. Sensors Actuators, B 2008;128:388–398.
31. Lidstrom ME, Meldrum DR. Nature Rev Microbiology 2003;1:158–164.
32. Molter TW, McQuaide SC, Suchorolski MT, Strovas TJ, Burgess LW, Meldrum DR, Lidstrom ME. Sensors Actuators B 2009;135:678–686.
33. Hong HG, Jiang M, Sligar SG, Bohn PW. Langmuir 1994;10:153–158.
34. Li L, Walt DR. Anal Chem 1995;67:3746–3752. [PubMed: 8644922]
35. Ramachandram B, Saroja G, Sankaran B, Samanta A. J Phys Chem B 2000;104:11824–11832.

36. Borisov SM, Wolfbeis OS. Chem Rev 2008;108:423–461. [PubMed: 18229952]
37. Zhao Y, Ye T, Chen H, Huang D, Zhou T, He C, Chen X. Luminescence. 200910.1002/bio.1182
38. McDonagh C, MacCraith BD, McEvoy AK. Anal Chem 1998;70:45–50.
39. Demas JN, DeGraff BA. Sens Actuators B 1993;11:35–41.
40. Ogurtsov VI, Papkovsky DB. Sens Actuators B 2006;113:917–929.
41. Klimant I, Ruckruh F, Liebsch G, Stangelmayer A, Wolfbeis OS. Mikrochim Acta 1999;131:35–46.
42. Wolfbeis OS, Offenbacher H, Kroneis H, Marsoner H. Mikrochimica Acta 1984;82:153–158.
43. McEvoy A, McDonagh C, MacGraith B. J Sol-Gel Sci Technol 1997;8:1121–1125.
44. Garcia-Fresnadillo D, Marazuela MD, Moreno-Bondi MC, Orellana G. Langmuir 1999;15:6451–6459.
45. Adronov A, Fréchet JMJ. Chem Comm 2000:1701–1710.
46. Choi MS, Yamazaki T, Yamazaki I, Aida T. Angew Chem Int Ed 2004;43:150–158.

Biographies

Yanqing Tian received his BS and MS degrees from Department of Organic Chemistry, Jilin University (China) in 1989 and 1992. In 1995, he received his Ph.D. degree in Polymer Chemistry and Physics from Jilin University. He worked at Jilin University, Sagami Chemical Research Center (Japan), Tokyo Metropolitan University, Tokyo Institute of Technology, Tokyo University of Science, and University of Washington. He is now working at the Center for Ecogenomics, Biodesign Institute at Arizona State University as a Research Scientist. His research interests include synthesis and application of optical sensors and block copolymers for biosensing, bioimaging and drug delivery.

Bradley R. Shumway received his BS degree in Molecular Biosciences and Biotechnology from Arizona State University in 2009. From 2008 to 2010 he has worked as a researcher for the Center for Ecogenomics at the Biodesign Institute at Arizona State University, focused on the development of optical sensors of oxygen and pH. He will commence medical education in 2010.

Cody Youngbull is an experimental physicist working on biological problems. Currently a research scientist in the Biodesign Institute at Arizona State University, he received his bachelor's degree in Physics from The Colorado College and his Ph.D. in Physics from the University of Washington in 2007. Cody's diverse research projects have included studying starquakes and remote sensing at Los Alamos National Laboratory, cellular automata at The Santa Fe Institute, and Raman spectroscopy at Arizona State University. Cody's expertise is on the development and characterization of ultrafast laser generated devices and nonlinear optical materials, especially as they apply to biological inquiry.

Yongzhong Li received his BS in agronomy and MS in plant science from Department of Agronomy, Jilin Agriculture University (China) in 1982 and 1985. In 2002, he received his Ph.D. degree in Biology from The University of Toledo, Ohio, USA. He worked at Jilin Academy of Agricultural Sciences, Kansas State University, Ohio State University, Northwestern University, University of Illinois at Chicago and Arizona State University. He is now working at NeoStem company as a Senior Research Scientist and Director of Stem Cell Research Laboratory. His research interests include cancer biology and stem cell therapy.

Roger Johnson has been a Research Scientist and Laboratory Manager in the Center for Ecogenomics in ASU's Biodesign Institute since 2006. Roger is responsible for overall management of daily research activities in the Center, and leads the cell CT research. He has over twenty years' experience in 3D micro CT, and is an expert in CT scanner design and construction, image reconstruction algorithms, and 3D image processing and analysis. Prior to

joining ASU, he was a tenured associate professor in Biomedical Engineering at Marquette University in Milwaukee, with appointments at the Medical College of Wisconsin (Departments of Biophysics and Radiology) and the Milwaukee VAMC Department of Physiology, where he built an x-ray microtomograph to study the lung microvasculature in animal models of pulmonary hypertension. Before moving to Marquette in 1996, he was Assistant Professor in Bioengineering and Radiology at The Ohio State University. Roger obtained his BA degree in German and chemistry from the University of Connecticut in 1979. This included a junior year abroad in Salzburg, Austria. From 1980 through 1987 he worked in the orthopedic implant field, both in industry and the hospital-based research setting. It was this pursuit that led him to the practice and the study of 3D medical imaging, first with light and electron microscopy, then using other modalities including CT, MRI, and PET. He returned to complete the Ph.D. in Bioengineering at the University of Washington from 1987 to 1995. For his dissertation research, he designed and built an x-ray microscope and x-ray microtomograph for point-projection data acquisition of biological specimens. Dr. Johnson is co-inventor of the cell CT and has seven patents including two on x-ray and two on optical microtomography.

Alex Jen is currently the Boeing-Johnson Chair Professor and Chair of the Materials Science and Engineering Department at the University of Washington. He also serves as the Director of the Institute of Advanced Materials and Technology. For his pioneering contributions in organic photonics and electronics, he was elected as a Fellow by several professional societies such as the American Association of the Advancement of Science (AAAS), the International Society of Optical Engineering (SPIE), the Optical Society America (OSA), and the American Chemical Society's Polymeric Materials Science & Engineering (PMSE) Division. He has co-authored more than 400 publications and 50 patents.

Deirdre Meldrum, Dean of the Ira A. Fulton Schools of Engineering at Arizona State University, is also director of the Center for Ecogenomics at the Biodesign Institute. In addition, Meldrum directs a National Institutes of Health Center of Excellence in Genomic Sciences called the Microscale Life Sciences Center. Her research interests include genome automation, microscale systems for biological applications, single cell technologies for understanding cancer and inflammation, ecogenomics, robotics and control systems. Before joining ASU in 2007, Meldrum was on the faculty of the University of Washington in Seattle since 1992, where she founded and directed UW's Genomation Laboratory. She is a member of the National Advisory Council for Human Genome Research, a Presidential Early Career Awardee for Scientists and Engineers (PECASE), fellow of the Institute of Electrical and Electronics Engineers (IEEE), and fellow of the American Association for the Advancement of Science (AAAS). She received her B.S. in Civil Engineering from University of Washington, her M.S. in Electrical Engineering from Rensselaer Polytechnic Institute, and her Ph.D. in Electrical Engineering from Stanford University.

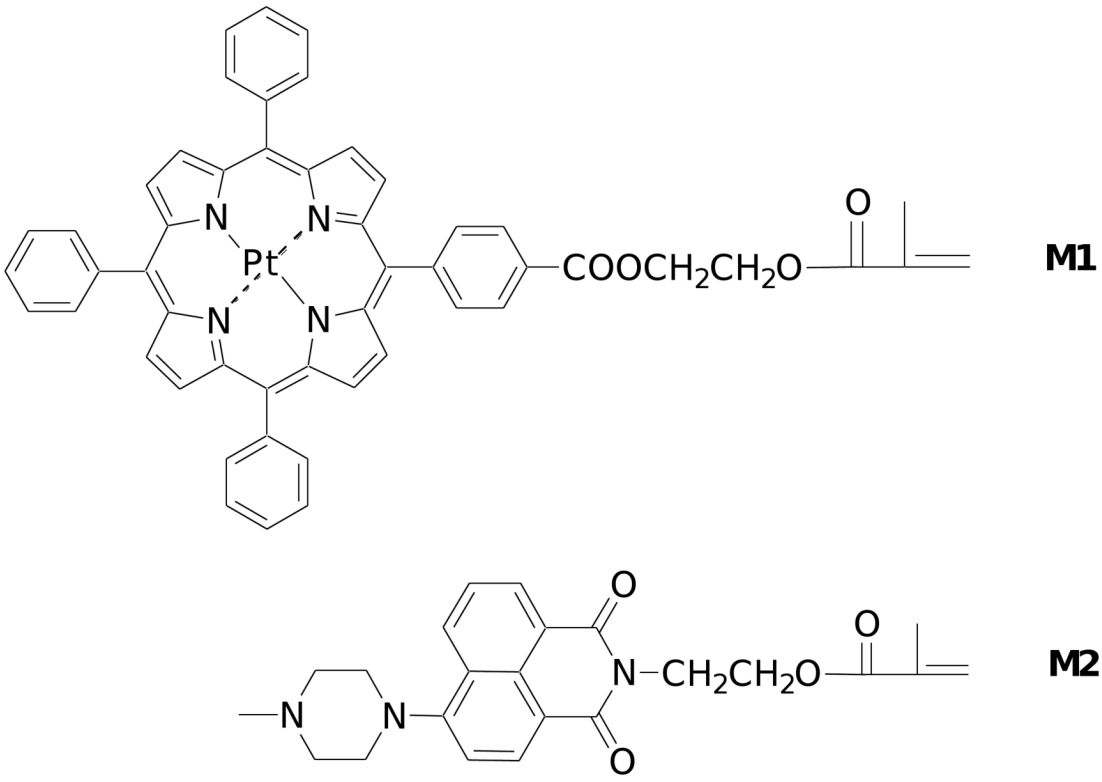

Figure 1.
Structures of **M1** and **M2**.

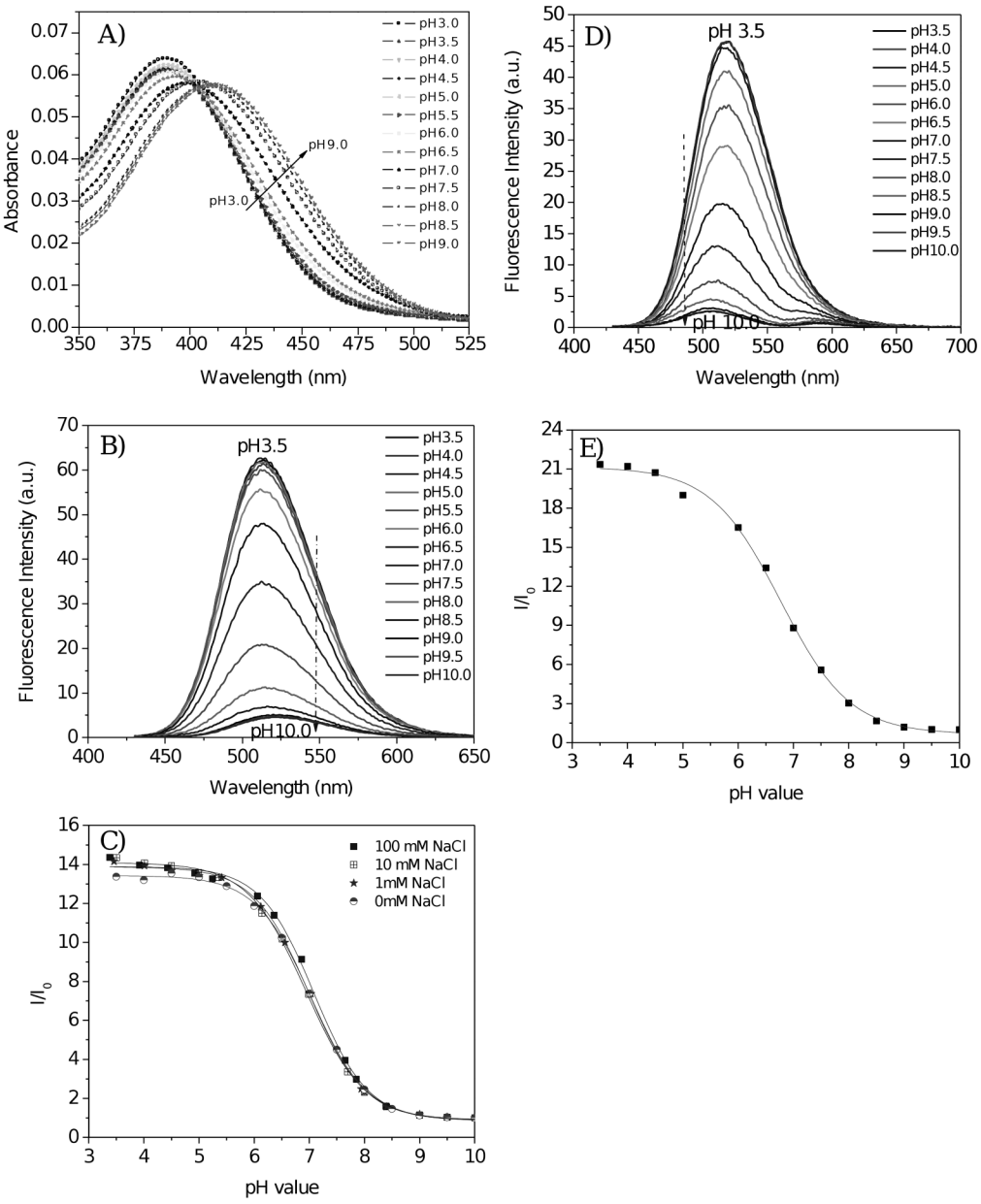

Figure 2.

A) Absorbance and B) emission of pH sensing membrane in B-R buffer at different pH values. C) Fluorescence intensity ratios at different salt concentrations. I_0 is the fluorescence intensity at 515 nm in pH 10.0 buffer. Fluorescence spectra were obtained using 405-nm excitation light. D) Fluorescence intensities of the pH sensing membrane in DMEM at different pH values. E) Fluorescence intensity ratios of figure D. I_0 is the fluorescence intensity at 515 nm in pH 10 DMEM. According to the sigmoidal plot, the pK_a is 6.82 with a R^2 of 0.997. The weak emission between 550 and 625 nm was due to autofluorescence of the medium.

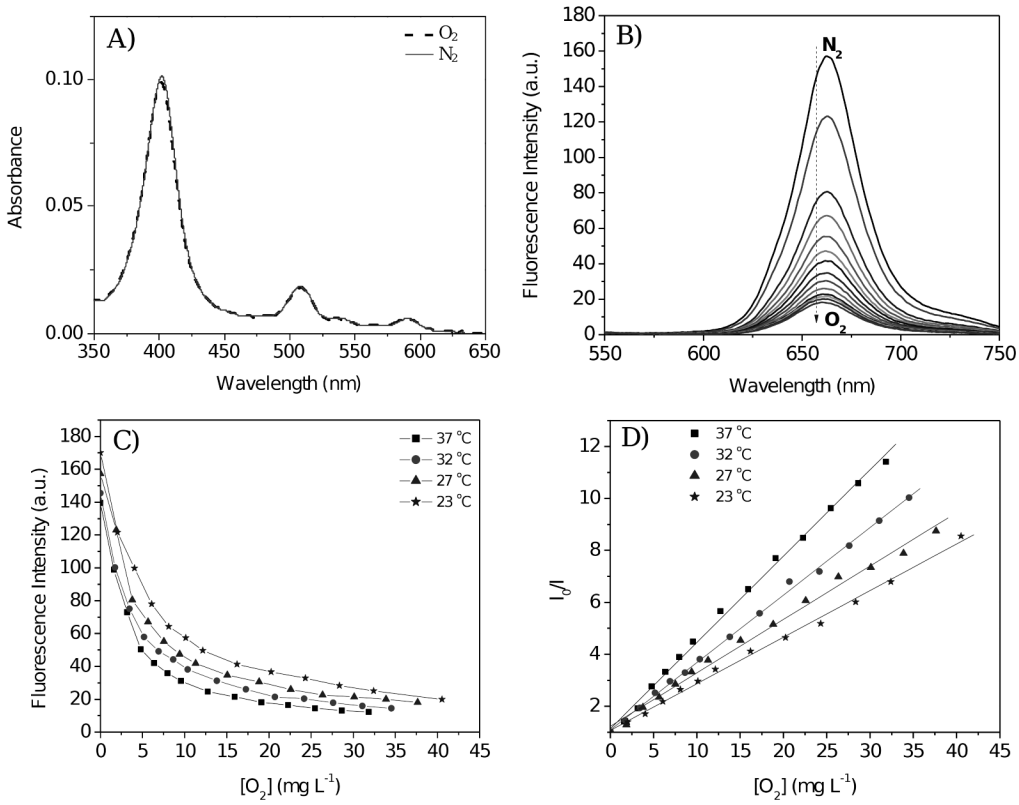

Figure 3.

A) Absorbance and B) emission of oxygen-sensing membrane in B-R buffer (pH 7.5) with different dissolved oxygen concentrations [O_2]; C) Temperature dependent emission intensities at 660 nm in pH 7.5 B-R buffer; D) Stern-Volmer curves at different temperatures. Fluorescence spectra were obtained using 405-nm excitation light.

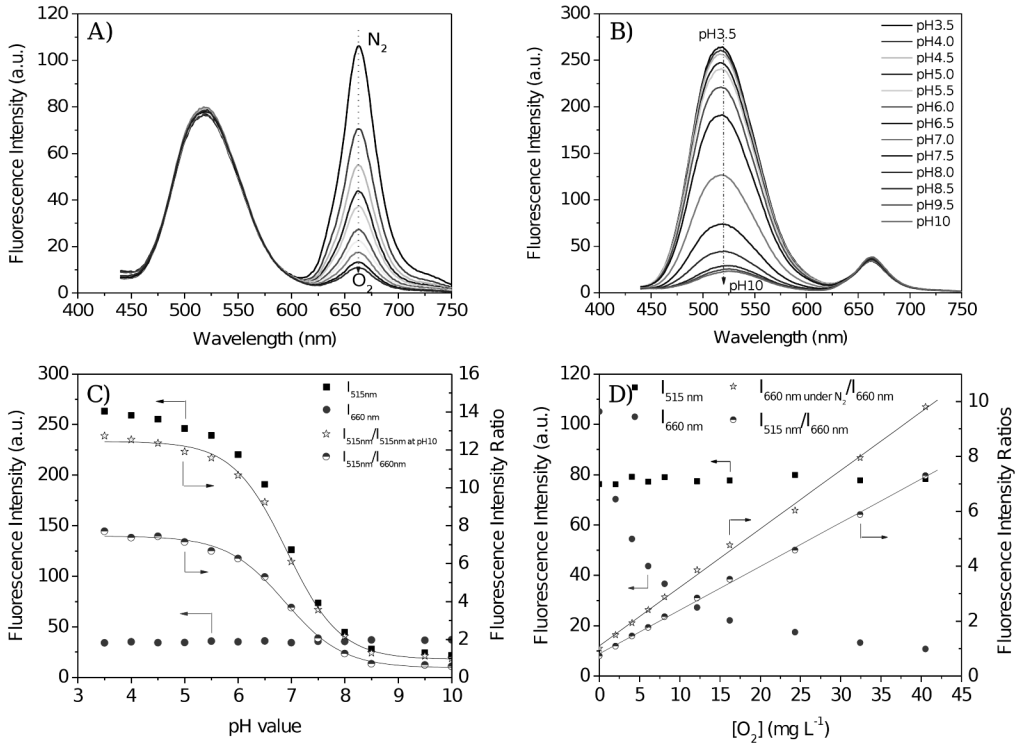

Figure 4.

Oxygen and pH responses of the dual-sensor. A) Measured in pH 7.5 B-R buffer with different dissolved oxygen concentrations [O_2]; B) Measured in air-equilibrated buffers, corresponding to oxygen partial pressure of 21 kPa or [O_2] of 8.6 mg L^{-1}. C) Intensity variations with pH under air-equilibrated buffers. D) Intensity variations in pH 7.5 B-R buffer with different DO concentrations [O_2]. Intensity ratio of $I_{515nm}/I_{515nm\ at\ pH\ 10}$ in Figure C was for pK_a determination using method A. I_{515nm}/I_{660nm} in Figure C was for pK_a determination using method C. $I_{660nm\ under\ N2}/I_{660nm}$ in Figure D was for K_{SV} determination using method B. I_{515nm}/I_{660nm} in Figure D was for K_{SV} determination using method D. pK_as were determined from the sigmoidal plots; K_{SV}s were determined from the Stern-Volmer equations.

Table 1

pK_a values and Stern-Volmer constants.[a)]

	pK_a from Method A [c)]	**pK_a from Method C** [c)]	**K_{SV} from Method B** [d)]	**K_{SV} from Method D** [d)]
pH sensor only [b)]	7.04 (0.999)			
Dual sensor [b)]	6.93 (0.998)	6.94 (0.996)	0.084 (0.997)	0.065 (0.999)
Oxygen senor only [b)]			0.074 (0.997)	

[a)] Correlation coefficient (R^2) in parentheses.

[b)] Experiments carried out at room temperature.

[c)] Experiments carried out in air-equilibrated buffers, corresponding to oxygen partial pressure of 21 kPa or [O_2] of 8.6 mg L^{-1}.

[d)] Experiments carried out at pH 7.5 and unit in kPa^{-1}.

Table 2

pH and pO_2 [a)] measured with dual-sensor membrane

	Set-point	Measured values method A	Measured values method C	Measured values method B	Measured values method D
pH [b)]	5.53[c)]	5.37 (-0.16)	5.42 (-0.11)		
	7.16[d)]	7.07 (-0.09)	7.14 (-0.02)		
	7.60 [d)]	7.63 (+0.03)	7.64 (+0.04)		
pO_2[e)]	5.1			4.6 (-0.5)	4.6 (-0.5)
	8.1			8.4 (+0.3)	8.2 (+0.1)
	10.1			9.7 (-0.4)	9.7 (-0.4)
	12.2			12.0 (-0.2)	12.5 (+0.3)
	15.2			14.6 (-0.6)	15.5 (+0.3)
	20.2			19.0 (-1.2)	20.7 (+0.5)

[(a)] pO_2 represents the oxygen partial pressure in kPa;

[(b)] Oxygen partial pressure of 21 kPa corresponding to $[O_2]$ of 8.6 mg L^{-1};

[c)] pH 5.53 solution composed of tris(hydroxymethyl) aminomethane and hydrochloride acid with 10 mM NaCl;

[d)] B-R buffers;

[e)] Measurements carried out in pH 7.5 B-R buffer.